MJSAT

Malaysian Journal of Science and Advanced Technology

journal homepage: https://mjsat.com.my/

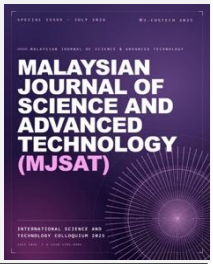

Potential of Silver Nanoparticles Fabricated from *Ananas comosus and Garcinia mangostana* Wastes as Co-catalysts in the Production of Biohydrogen

Zainab Razali*[1], Nor Alia Syakirah Azman[1], Nur Maisarah Sarizan[1], Nur Fazrina Samsuri[1], Roejhan Md Kawi[2] and Norrizah Jaafar Sidik[3]

[1]*Faculty of Applied Sciences, Universiti Teknologi MARA, Perlis Branch, Arau Campus, 02600 Arau, Perlis.*
[2]*Faculty of Electrical Engineering & Technology, Universiti Malaysia Perlis, Pauh Putra Campus, 02600 Arau, Perlis, Malaysia.*
[3]*Faculty of Applied Sciences, Universiti Teknologi MARA, 40450 Shah Alam, Selangor, Malaysia.*

KEYWORDS

AgNPs
Ananas comosus
Garcinia mangostana
Biohydrogen
Chronoamperometry

ARTICLE HISTORY

Received 22 November 2025
Available online 21 August 2026

ABSTRACT

The increasing demand for clean and sustainable energy sources has driven interest in biohydrogen production, particularly through environmentally friendly approaches such as the utilization of silver nanoparticles (AgNPs) synthesized from agricultural wastes. Therefore, this study focuses on the green synthesis of silver nanoparticles (AgNPs) using *Ananas comosus* (pineapple) and *Garcinia mangostana* (mangosteen) peel extracts as eco-friendly bioreducing and stabilizing agents, and their catalytic performance in biohydrogen production. The synthesized AgNPs were characterized using UV-Vis spectroscopy and Fourier Transform Infrared (FTIR) spectroscopy. The UV-Vis spectra confirmed nanoparticle formation, with Surface Plasmon Resonance (SPR) peaks observed between 400–460nm while FTIR analysis indicated the presence of functional groups to support the involvement of plant phytochemicals in the reduction and stabilization of AgNPs. Catalytic efficiency was evaluated via chronoamperometry and by using 0.01 M $AgNO_3$ as a precursor. Results showed that AgNPs synthesized with *A. comosus* at 0.1 g/mL exhibited the highest biohydrogen yield (0.0112ml), while *G. mangostana* at 0.15 g/mL also demonstrated notable hydrogen generation (0.0747ml), though the current signal

1. INTRODUCTION

As the world expands with increased environmental problems and the shift towards eco-friendly energy, silver nanoparticles (AgNPs) are an effective and innovative tool across various fields of science [1]. The specific properties of these nanoparticles include morphology, function, and surface characteristics that include high surface area to volume ratio, high catalytic activity, and high antimicrobial ability which makes them very useful for many applications [2]. Out of all the synthesis approaches, plant-mediated synthesis of AgNPs has gained much attention because of its environmentally benign character, economical, and compliance with green chemistry protocol [3]. This green synthesis approach accordingg to Marouš ek [4], capable reduces hazardous chemicals or toxic reductants in the synthesis process and provides biocompatible nanoparticles due to the use of phytochemical compounds extracted from plants including advances demonstrate the contemporary place and importance of AgNPs in and technology.

Biohydrogen which is obtained through biochemical reactions as stated by Azevedo et al. [5] can be used as a source of energy that will replace the use of fossil fuels due to its large potential as a form of energy. However, the use of biohydrogen is constrained by factors such as low production standards and excessive cost of production [6]. This has been supported by Thirumalaivasan et al. [3] who show that the synthesis of AgNPs is favorable for hydrogen evolution reactions and photocatalytic water splitting. Thus, the incorporation of green synthesis methods along with plant-based AgNPs as co-catalyst in the biohydrogen production systems also improves the reaction rate steadily and this bifrontal approach cascades from advanced nanotechnology to renewable energy sources, which provides a sustainable solution to eliminate the ongoing energy problem [3].

*Corresponding author:
E-mail address: Zainab Razali < zainab215@uitm.edu.my >
https://doi.org/10.56532/mjsat.v6iS1.781

According to Iravani et al. [1], the green synthesis of AgNPs through plant extracts takes advantage of these extracts that contain phytochemicals that would improve catalytic performance [1]. To this, the project scope entails the characterization of the synthesized AgNPs, determining the efficiency of the synthesized AgNPs as co-catalysts in the biohydrogen process, and the assessment of the green synthesis approach to the environment [2]. In the previous study by Maroušek [4], the aims are to solve two problems simultaneously which are to minimize the toxic effects of chemical synthesis on the environment during the synthesis process of biohydrogen and to make the production process economically viable. Moreover, according to Maroušek [4] and Thirumalaivasan et al. [3], the project seeks to inform the implementation of sustainable environmental policies and principles in the generation of clean renewable energy, in considering the reduction of greenhouse gases during the development of technologies toward energy sustainability.

The findings from this research are expected to contribute significantly to advancing green synthesis technologies and their role in sustainable energy generation [7]. According to Bhosale and Bhanage [8], by using sustainable routes in nanotechnology synthesis can enhance biohydrogen production, where plant-based AgNPs have the potential to improve the system. The biosynthesis approach by using water waste materials from plants is widely used as it is proven to be an environmentally friendly and cost-effective method [9].

Green-synthesized silver nanoparticles (AgNPs) are increasingly popular, but they still have several drawbacks, particularly their inconsistent characteristics and limited use in biohydrogen systems. The majority of research focuses less on energy-related applications and more on synthesis and antibacterial qualities. Although the synthesis of biohydrogen through biological processes, such as dark fermentation, seems promising, it is often limited by low yields and inefficient electron transport [10]. To increase hydrogen production, efficient and long-lasting catalytic techniques are therefore required.

In this regard, there is still a lack of research on the application of plant-mediated AgNPs made from fruit peel waste as co-catalysts. Thus, this paper examines how AgNPs can be synthesized using the peel wastes of *Ananas comosus* and *Garcinia mangostan*a and how these nanoparticles can be used to enhance the process of biohydrogen production and presents a sustainable approach to the use of renewable energy alongside the valorization of waste.

This work described and evaluated AgNPs prepared using plant extracts in the production of biohydrogen catalytically. This study aims to understand the relationship between the properties of the nanoparticles and their ability to enhance the hydrogen generation. The strategy aligns with the principles of sustainable nanotechnology, which include the need to use natural resources as generated to create clean energy technologies [11].

2. METHODOLOGY

2.1 Preparation of peel extracts

The preparation of peel extracts from *Ananas comosus* (pineapple) and *Garcinia mangostana* (mangosteen) followed a green synthesis approach to harness their natural reducing agents based on Ismail et al. [12]. The collected fruit peels were washed, dried at 50°C, and ground into fine powder using a mechanical grinder. Aqueous extraction was performed by mixing each peel powder with distilled water at different weights and volume to form different concentrations, which are 100 mg/mL, 150 mg/mL, and 200 mg/mL. Then, the mixture was heated on a hotplate at 70°C for 10 minutes. After cooling to room temperature, it was filtered with Whatman No. 1 filter paper to remove any residues and stored at 4°C in an amber glass bottle until further use.

1.1 Synthesizing AgNPs using Ananas comosus and Garcinia mangostana peel extracts

The synthesis of silver nanoparticles (AgNPs) using *A. comosus* and *G. mangostana* peel extracts was performed by preparing a 0.01 M aqueous silver nitrate ($AgNO_3$). A total of 0.255g of the $AgNO_3$ powder was dissolved with 150 mL dH_2O. The $AgNO_3$ acts as a precursor while peel extracts as a reducing agent to synthesize AgNPs. A mixture consisting of 20 mL of 0.01 M aqueous $AgNO_3$ and 2 mL of peel extracts was prepared at different concentrations, which are 100 mg/mL, 150 mg/mL, and 200 mg/mL. Each mixture was transferred into separate Erlenmeyer flasks and heated in a water bath at 60°C for 60 minutes. The colour changes were observed and recorded at 10-minute intervals throughout the reaction. The reduction of $AgNO_3$ to silver ions (Ag^+) indicated by a visible colour change from colourless to brown. Then, centrifuged at 5000 rpm for 30 minutes and supernatant was discarded. The resulting pellet was resuspended in deionized water, and the centrifugation process was repeated to remove any residual substances adsorbed on the surface of the nanoparticles and the resulting pellet was collected. The pellet then dried and stored in small petri dishes. The dried form of the AgNPs samples were analyzed through Fourier-transform infrared (FTIR) spectroscopy to determine their functional groups.

The mixture was centrifuged at 5000 rpm for 30 minutes, and the supernatant was discarded. The resulting pellet was washed with deionized water and centrifuged repeatedly to remove unreacted precursors and residual phytochemicals. This purification step ensured that the obtained AgNPs were free from excess impurities before being used for further characterization and biohydrogen experiments.

2.3 Characterization

2.3.1 UV-Visible spectrophotometer (UV-Vis)

According to Vasyliev et al. [13], the formation of AgNPs was verified using a UV-Vis spectrophotometer by monitoring the surface plasmon resonance (SPR) peak. For this analysis, the mixtures of plant extracts at different concentrations with 0.01 M aqueous $AgNO_3$ were placed in cuvettes with distilled water. The absorbance spectra were recorded within the wavelength scanning range of 300–600 nm. A characteristic peak between 400 and 460 nm was identified that indicates the presence of AgNPs.

2.3.2 Fourier Transform Infrared spectroscopy (FTIR)

FTIR analysis was then carried out to determine the functional groups involved in the reduction, stabilization, and capping of AgNPs synthesized from *A. comosus* and *G. mangostana* peel extracts. As described by Veerasamy et al.

[12], the control samples which is 0.01 M of aqueous $AgNO_3$ allowing for the identification of the native phytochemical functional groups. The test samples were synthesized AgNPs obtained after the reduction of $AgNO_3$ by the peel extracts. These samples undergo centrifugation at 5000 rpm for 10 minutes, after that the supernatant discarded, and the resulting nanoparticles pellet was washed, dried, and analyzed using FTIR. The FTIR spectra were recorded within the wavenumber range of 4000–400 cm^{-1} to detect specific functional groups involved in nanoparticles stabilization. Peaks expected in the region 3200–3500 cm^{-1} correspond to hydroxyl (-OH) functional groups that play a key role in stabilizing AgNPs, while peaks between 1600–1700 cm^{-1} indicate carbonyl (C=O) groups that suggest the presence of flavonoids and other reducing agents [13], while ether (C–O) stretching vibrations within 1000–1300 cm^{-1} indicate the involvement of phenolics compounds [14]. Peaks appearing between 500–800 cm^{-1} will confirm the formation of AgNPs through the presence of Ag–O or Ag–N bonds [7]. The spectral differences between the control and test samples will provide insights into the specific phytochemical compounds responsible for AgNP synthesis and stabilization.

2.4 Biohydrogen production using Ananas comosus and Garcinia mangostana

To evaluate the catalytic efficiency of biosynthesized silver nanoparticles (AgNPs) in biohydrogen production, a basal fermentation medium was prepared in beaker by dissolving 10 g/L glucose, 2 g/L yeast extract, 10 g/L peptone, 0.5 g/L potassium dihydrogen phosphate (KH_2PO_4), 1 g/L dipotassium phosphate (K_2HPO_4) and 0.25 g/L magnesium chloride hexahydrate ($MgCl_2 \cdot 6H_2O$) in 1L of distilled water. This solution was autoclaved at 120 °C for 15 minutes to ensure sterility. The silver nanoparticles (AgNPs) used were synthesized using plant peel extracts and 0.01M of aqueous silver nitrate, and prepared at varying concentrations of 100 mg/mL, 150 mg/mL, and 200 g/mL. After the biosynthesis reaction was completed using a water bath at 60°C for 60 minutes, 2 mL of the AgNP-silver nitrate mixture were added to 43 mL of the prepared basal medium and 5 mL of anaerobic sludge was added to achieve a final working volume of 50 mL.

The fermentation mixtures were placed in 100 mL conical flasks, sealed with 1.0 mL of paraffin oil to create an anaerobic layer, and the flask mouths are securely wrapped with parafilm and aluminum foil to prevent gas leakage. The flasks were incubated in a shaking incubator at 35 °C and 130 rpm for 72 hours to allow for optimal microbial activity and hydrogen production. After fermentation, the hydrogen gas produced was analyzed electrochemically using a Metrohm Autolab PGSTAT NOVA 1.11 software system via the chronoamperometry technique followed from previous study by Gao et al. [15], the electrochemical setup used 0.1 M sulfuric acid (H_2SO_4) as the electrolyte. The working electrode was a glassy carbon electrode, the reference electrode was Ag/AgCl, and the counter electrode was platinum. A fixed potential of -1.3 V was applied during the measurement to facilitate the reduction process and evaluate hydrogen evolution via catalytic activity of the synthesized AgNPs.

2. RESULT AND DISCUSSION

2.1 Visual observation of silver nanoparticle formation using Ananas comosus and Garcinia mangostana peel extracts

The solutions turned slowly yellowish to light brown and darker brown respectively after 60 minutes depending on the concentration of the *A. comosus* peel extract (100, 150 and 200 mg/mL). *G. mangostana* extract mixture, conversely, became brown more quickly and had a darker color within the same time. The cause of this difference in color intensity is likely to be due to variations in their phytochemical contents which are known to reduce Ag + ions to Ag 2 nanoparticles, including phenolics, flavonoids, and vitamin C.

The same color variation has been reported in earlier studies [16], whereby the interaction of pineapple peel extract with silver nitrate solution gave a colorless-to-brown color shift, which increased with time and extract concentration thus indicating the formation of nanoparticles. Ismail et al. [12] assert that the brown color is due to the excitation of surface plasmon resonance (SPR), which is one of the optical properties of AgNPs. The difference in color intensity is attributed to the difference in the phytochemical composition of the two fruit peels. As mentioned in previous studies, such substances as ascorbic acid, flavonoids, and phenolics are stabilizing and reducing agents in green synthesis [17].

The presence of the brown color after an hour shows that the reduction process was complete and that the AgNPs formed were stable throughout the period of observation. The successful biosynthesis was corroborated by spectroscopic methods which is first indicated by this visual confirmation.

3.2 Characterization of silver nanoparticles

The UV-Vis spectroscopy results confirm the successful synthesis of AgNPs using *A. comosus* and *G. mangostana* peel extracts, as evidenced by characteristic surface plasmon resonance (SPR) absorption peaks in the range of 400–460 nm. The absorbance spectrum was recorded over the scanning range of 300–600 nm, which covers the near-UV to visible light range. Usually, the SPR peaks observed in this study fall within the region of the visible light, supporting the typical optical response of metallic silver nanoparticles. As shown in Table 1, the absorption maxima for *A. comosus*-derived AgNPs with different concentrations of 100 mg/mL, 150 mg/mL, and 200 mg/mL were observed at 446 nm (0.6074 a.u.), 449 nm (0.9589 a.u.), and 451 nm (1.1290 a.u.).

While for *G. mangostana*-derived AgNPs with similar concentrations, the SPR peaks were observed at 440 nm (2.5914 a.u.), 440.5 nm (2.5914 a.u.), and 441.5 nm (2.5710 a.u.). These results are in alignment with Abdelbasir et al. [18] and Rahman et al. [19], who reported that AgNPs typically exhibit SPR bands between 400–460 nm, confirming the formation of metallic silver nanoparticles. The peaks in *G. mangostana* samples (440–441.5 nm) compared to *A. comosus* samples (446–451 nm) suggest that the former may produce smaller and more uniformly distributed AgNPs, as also supported by Alabdallah & Hasan [20]. Besides, the increase in absorbance intensity from 100 to 200 mg/mL in both extracts reflects a higher nanoparticle concentration, implying more efficient bioreduction of silver ions (Ag^+) with increased extract concentration. This observation is consistent with the findings of Gomes et al. [21], which reported that higher extract concentrations can improve nanoparticles yield. In the

case of *G. mangostana*, the SPR peaks were narrower and more symmetrical, indicating a fairly uniform nanoparticle size distribution. The uniformity observed may be linked to phytochemicals such as phenolics, flavonoids, and organic acids found in both plant extracts, which serve as natural reducing and stabilizing agents. These compounds likely played a role in promoting the quick and stable formation of AgNPs.

Table 1. UV-Vis Absorption Spectrum of AgNPs Synthesized using Different Concentrations of Peel Extracts

Extract Source	Concentration (mg/mL)	SPR Peak Wavelength (nm)	Absorbance (a.u.)
Ananas comosus	100	446.0	0.6074
	150	449.0	0.9589
	200	451.0	1.1290
Garcinia mangostana	100	440.0	2.5914
	150	440.5	2.5914
	200	441.5	2.5710

FTIR spectroscopy was employed to identify the functional groups involved in the reduction, capping, and stabilization of AgNPs synthesized from *A. comosus* and *G. mangostana* peel extracts. The spectra were scanned across the range of 4000 to 400 cm^{-1}, which revealed characteristic absorption peaks indicating the presence of phytochemical compounds involved in nanoparticle formation.

The control sample as shown in Figure 1, containing only 0.01 M $AgNO_3$ exhibited FTIR peaks at 1387.5 cm^{-1} and 834.43 cm^{-1}. These peaks do not correspond to the characteristic functional groups typically involved in nanoparticle synthesis, such as O–H, C=O, or C–O vibrations. The absence of these functional groups in the control confirms that no phytochemicals were present to reduce or cap the Ag^{+} ions. So, no significant bioreduction or stabilization occurred, which shows that the critical role of plant-derived biomolecules in the formation of AgNPs. This further validates the interaction observed in the plant-mediated AgNP samples, where functional group shifts and intensity changes were clearly linked to the nanoparticle synthesis process.

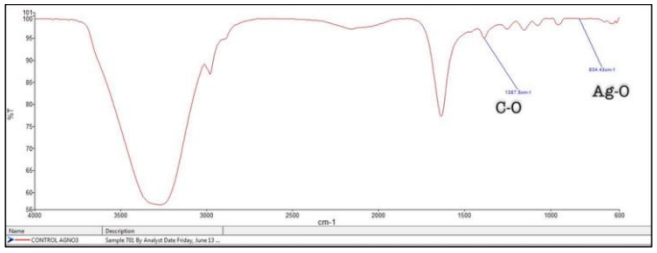

Fig. 1. FTIR Spectrum of 0.01M $AgNO_3$

From Figure 2, Figure 3, and Figure 4 for *A. comosus*-derived AgNPs, the FTIR spectra showed peaks at 3275.17 cm^{-1}, 1639.80 cm^{-1}, and 1247.2 cm^{-1} for 100 mg/mL; 3253.33 cm^{-1} , 1633.82 cm^{-1} , and 1244.87 cm^{-1} for 150 mg/mL; 3266.32 cm^{-1}, 1633.34 cm^{-1}, and 1249.78 cm^{-1} for 200 mg/mL. These peaks of 3200–3500 cm^{-1} correspond to the presence of O-H stretching that indicate the hydroxyl groups, 1600–1700 cm^{-1} correspond to C=O stretching that indicate carbonyl groups and 1000–1300 cm^{-1} correspond to C–O stretching that suggests the presence of phenolics or esters.

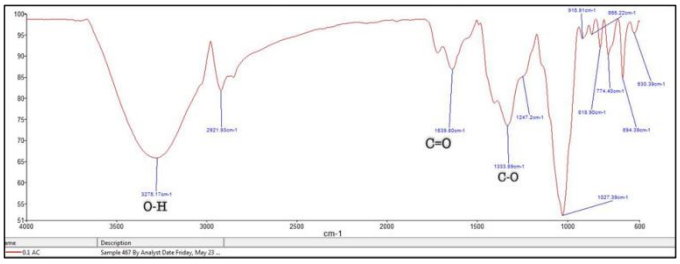

Fig. 2. FTIR Spectrum of AgNPs from *A. comosus* Peel Extract at 100 mg/mL

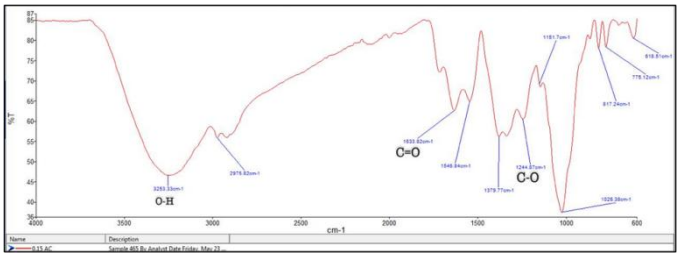

Fig. 3. FTIR Spectrum of AgNPs from *A. comosus* Peel Extract at 150 mg/mL

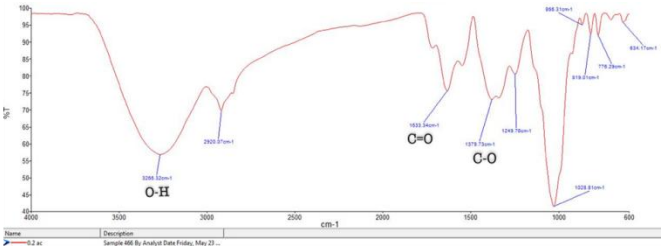

Fig. 4. FTIR Spectrum of AgNPs from *A. comosus* Peel Extract at 200 mg/mL

For *G. mangostana*-derived AgNPs, the observed FTIR peaks as we can see in Figure 5, Figure 6, and Figure 7 were 3199.49 cm^{-1}, 1611.51 cm^{-1}, and 1311.00 cm^{-1} for 100 mg/mL; 3299.5 cm^{-1}, 1699.2 cm^{-1}, and 1154.4 cm^{-1} for 150 mg/mL; 3198.4 cm^{-1}, 1603.34 cm^{-1}, and 1254.43 cm^{-1} for 200 mg/mL also correspond similar as the functional group of *A. comosus* except for the 1200–1600 cm^{-1} attributed to aromatic ring vibrations characteristic of xanthones, which are major active compounds in *G. mangostana*.

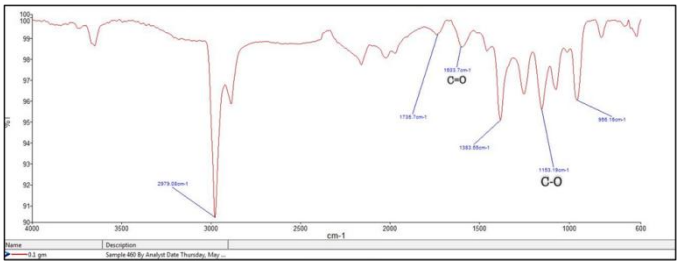

Fig. 5. FTIR Spectrum of AgNPs from *G. mangostana* Peel Extract at 100 mg/mL

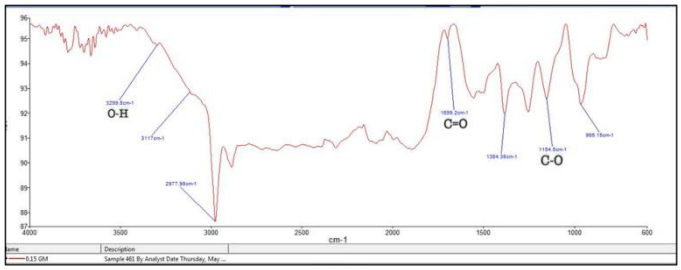

Fig. 6. FTIR spectrum of AgNPs from *G. mangostana* peel extract at 150 mg/mL

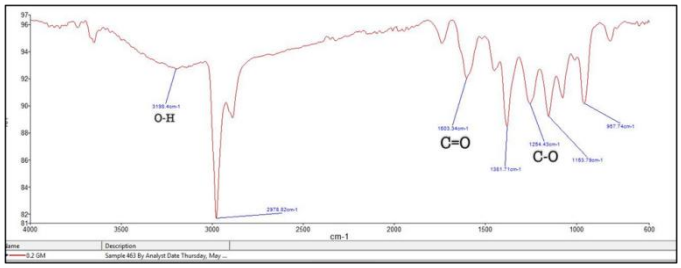

Fig. 7. FTIR spectrum of AgNPs from *G. mangostana* peel extract at 200 mg/mL

Phytochemical reaction with silver ions was verified by the FTIR spectra of AgNPs that were produced in the presence of the A. comosus and G. mangostana extracts which exhibited evident variations in the significant functional groups in the AgNPs than those that typically occur in plant extracts. For instance, a carbonyl stretching (C=O) vibration in A. comosus changed from 1639.80 cm^{-1} (at 100 mg/mL) to 1633.34 cm^{-1} (at 0.2 g/mL), whereas the carbonyl vibration band in G. mangostana changed from 1611.51 cm^{-1} in the 100 mg/mL extract to 1603.34 cm^{-1} in the AgNPs made at 200 mg/mL. This decrease is in line with C=O stretching, implying that phenolics or esters could have been involved in the reduction of silver ions and stabilization of the formed nanoparticles.

These functional groups are often provided by flavonoids, tannins and other plant-based compounds, which have the ability to donate electrons. The shift observed at the peak confirmed the formation of nanoparticles via reaction between Ag+ ions and carbonyl-containing chemicals. The two samples had general bands at the range of 3200 - 3500 cm -1, which is linked to OH stretching vibrations, commonly present in polyphenols and alcohols. According to Vasyliev et al. [13], these groups are reported to be reducing and capping agents in green synthesis. Although the absence of a color indicates the absence of any Ag-O or Ag-N bonding, the ether (C-O) stretching vibrations at the 1000 - 1300cm -1 area indicate the existence of phenolic compounds [14], although bands at the 500-800cm -1 area may indicate the existence of Ag-O or Ag-N bonds. Figure 1 showed major peaks at 1387.5 cm -1 and 834.43 cm -1, which were not found in the synthesized AgNP samples, in the control FTIR spectrum of 0.01 M AgNO -1. This proves that the functional groups in the AgNP spectra were not as a result of the silver precursor but the plant extracts.

The absence of peaks related to nitrate shows that silver ions were successfully reduced and incorporated into nanoparticles. The presence of green-synthesised silver nanoparticles (AgNPs) was established through UV-Vis and FTIR analysis of plant extracts indicating that they can be used in bioavailability [22].

The current work did not involve advanced imaging methods such as Transmission Electron Microscopy (TEM) and Scanning Electron Microscopy (SEM) that are commonly used to identify nanoparticle morphology and size distribution because of instrumental constraints. However, FTIR analysis and UV-Vis spectroscopy offered adequate initial proof of the creation of nanoparticles and the participation of functional groups. Also, it has been demonstrated by previous studies that the alteration of functional groups and unique surface plasmon resonance (SPR) peaks can be regarded as reliable indicators of successful nanoparticle production. Therefore, future work will incorporate SEM/TEM analysis to further validate particle morphology and size distribution.

3.3 Evaluation of catalytic efficiency of silver nanoparticles synthesized from Ananas comosus and Garcinia mangostana in biohydrogen production

The activity of the catalytic efficiency is measured using chronoamperometry techniques. In this method, the hydrogen gas was generated by using the electrochemical Hydrogen Evolution Reaction (HER), and a constant potential was used. On the working electrode surface, the protons (H+) are reduced to molecular hydrogen (H_2), and the resulting current is monitored time-dependent. In this research, chronoamperometry was conducted with the help of the Autolab NOVA 1.11 software where a constant potential of -1.3 V was used, which is enough to initiate HER. The availability of biosynthesized silver nanoparticles (AgNPs) enhances this reaction by providing active catalytic sites of proton reduction. AgNPs derived using peel extracts of Garcinia mangostana and *A. comosus* at different concentrations (100, 150, and 200 mg/mL) were examined in their capacity to catalyze the growth of hydrogen gas.

The catalytic effect of the biosynthesized silver nanoparticles was confirmed by conducting a control experiment in which AgNO 3 solution of 0.01 M was used without any fruit extract. Silver nitrate (AgNO 3) itself did not have the necessary catalytic power to catalyze hydrogen evolution at the potential of -1.3 V, as shown by the chronoamperometric response in Figure 8, which indicated negligible current during the 300-second period. This observation supports the concept that biogenically reduced AgNPs, produced using the peels of *A. comosus* and *G. mangostana*, can be used to enhance catalytic performance. The control establishes a reliable foundation, which validates the fact that the bioactive elements in the fruit extracts are imperative in the formation of nanoparticles and the consequent production of hydrogen.

AgNO3 can be used as a control to define the catalytic effect of silver ions and biosynthesized AgNPs. The low current value shows that the enhanced hydrogen evolution is due to the surface catalytic properties and nanoparticles structure rather than the existence of silver ions.

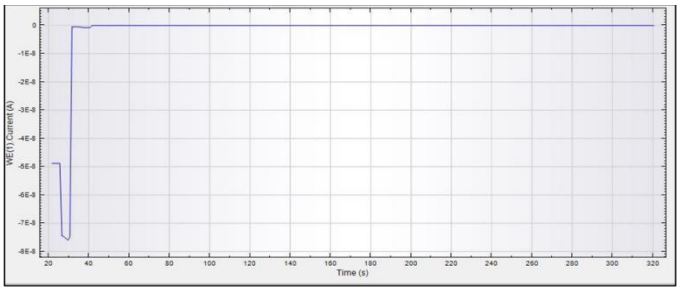

Fig. 8. Chronoamperometric graph for 0.01M $AgNO_3$

As shown in Figures 9, Figure 10 and Figure 11, the chronoamperometric graphs for *A. comosus* displayed clear steady-state current profiles for all tested concentrations. At 100 mg/mL, the steady-state current was approximately -3.0×10^{-4} A, indicating noticeable hydrogen generation activity. While the concentration of *A. comosus* at 150 mg/mL and 0.2 g/mL, the current decreased significantly to around -1.0×10^{-5} A and -7.5×10^{-6} A, respectively. This suggests that increasing the concentration beyond 100 mg/mL did not further enhance catalytic activity and may have resulted in reduced efficiency due to surface saturation.

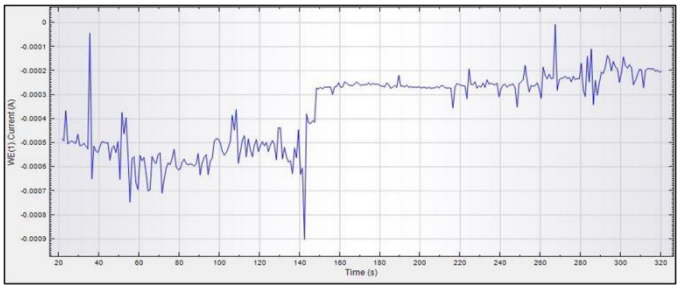

Fig. 9. Chronoamperometric graph for biohydrogen production using AgNPs synthesized from *A. comosus* peel extract at 100 mg/mL

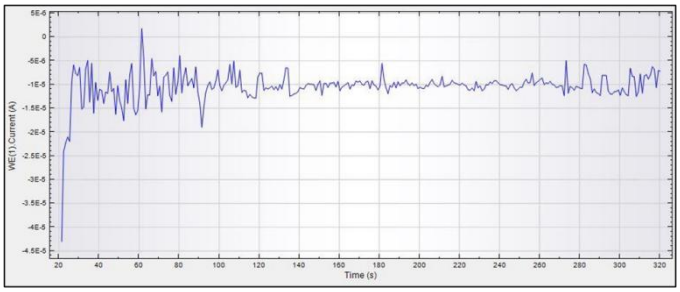

Fig. 10. Chronoamperometric graph for biohydrogen production using AgNPs synthesized from *A. comosus* peel extract at 150 mg/mL

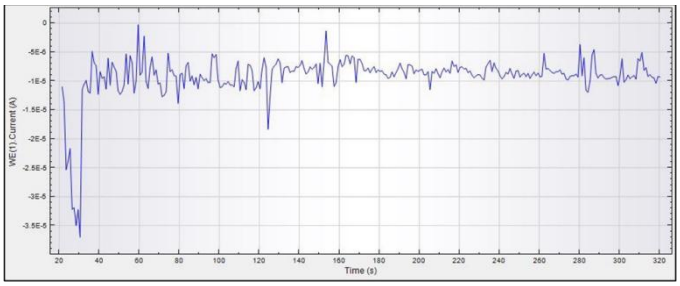

Fig. 11. Chronoamperometric graph for biohydrogen production using AgNPs synthesized from *A. comosus* peel extract at 200 mg/mL

Next, for *G. mangostana* samples, as shown in Figures 12, Figure 13, and Figure 14, the chronoamperometric graphs showed a minimal current activity. At 100 mg/mL and 200 mg/mL appeared mostly flat with currents near 0 A, closer inspection suggests the presence of very low and unstable current signals that is considered as electrochemical noise. These small fluctuations, although minimal, indicate that a limited amount of hydrogen was still generated. But for 150 mg/mL the current showed strong catalytic activity compared to 100 mg/mL and 200 mg/mL. The observed negative currents in the chronoamperometric graphs are a direct indicator of HER activity, with higher negative current values corresponding to increased hydrogen production.

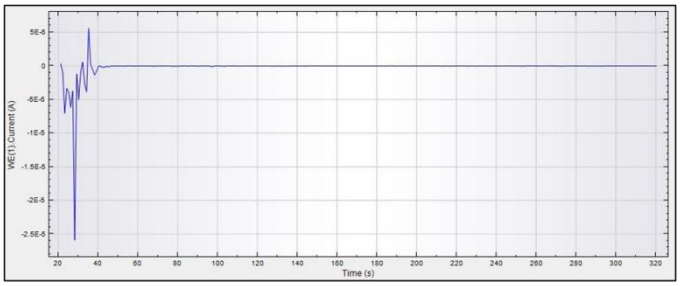

Fig. 12. Chronoamperometric graph for biohydrogen production using AgNPs synthesized from *G. mangostana* peel extract at 100 mg/mL

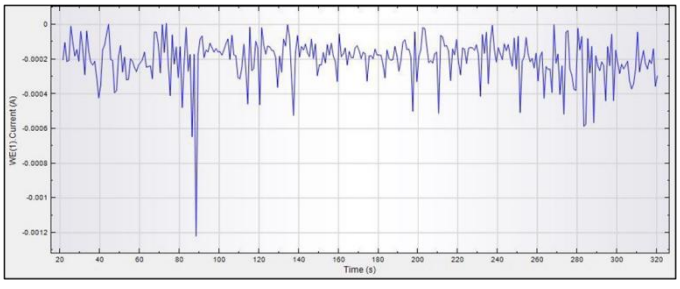

Fig. 13. Chronoamperometric graph for biohydrogen production using AgNPs synthesized from *G. mangostana* peel extract at 150 mg/mL

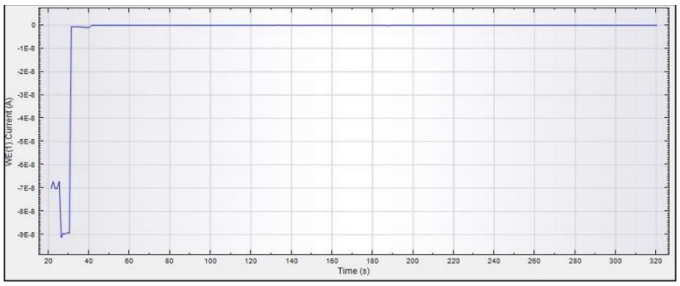

Fig. 14. Chronoamperometric graph for biohydrogen production using AgNPs synthesized from *G. mangostana* peel extract at 200 mg/mL

From chronoamperometric measurements, quantitative data can be obtained as shown in Tables 2 and 3, such as the total charge (Q), moles of hydrogen gas produced and the corresponding volume of H_2 that can provide a deeper insight into the catalytic performance of biosynthesized AgNPs from *A. comosus* and *G. mangostana* extracts.

The total charge (Q) generated during the chronoamperometry experiment was calculated using the equation:

$$Q = I \times \Delta t \quad (1)$$

where I is the steady-state current (in amperes) and Δt is the time =300s

The number of moles of hydrogen gas (mol H_2) was determined based on Faraday's law:

$$mol\ H_2 = Q/2F \quad (2)$$

Where F is the Faraday constant (96485 C/mol), and the factor of 2 accounts for the two electrons required per molecule of hydrogen evolved.

The volume of hydrogen gas was then calculated using the molar volume at NTP (24.0 L/mol):

$$Volume\ H_2 = mol\ H_2 \times 24.0\ L/mol \quad (3)$$

For *Ananas comosus* as shown in Table 2, the highest hydrogen production was observed at a concentration of 100 mg/mL, with a steady-state current of -3.0×10^{-4} A, resulting in a total charge of 0.09 C, equivalent to 4.66×10^{-7} mol of H_2 and a volume of hydrogen is 0.0112 mL. As the concentration increased to 150 mg/mL and 200 mg/mL, hydrogen production decreased indicate by lower current and charge values. This trend may be attributed to nanoparticle aggregation and potential microbial inhibition at higher extract concentrations. At elevated concentrations, nanoparticles tend to agglomerate, reducing their effective surface area and limiting catalytic activity. Additionally, excessive nanoparticle concentration may exert toxic effects on microbial communities involved in fermentation, thereby reducing hydrogen production efficiency. Similar observations have been reported in previous studies [23], where nanoparticle overloading negatively impacted catalytic and biological performance.

Table 2. Hydrogen production from *Ananas comosus* AgNPs

Extract/ Concentration (mg/mL)	*Ananas comosus*		
	100	*150*	*200*
Steady current, I (A)	-3.0×10^{-4}	-1.0×10^{-5}	-7.5×10^{-6}
Total electric charge, Q (C)	0.0900	0.0030	0.00225
Moles of H_2 (mol)	4.66×10^{-7}	1.56×10^{-8}	1.17×10^{-8}
Volume of H_2 (mL)	0.01120	0.000374	0.00028

Next for *Garcinia mangostana* showed in Table 3, the peak catalytic activity at 150 mg/mL, with a significantly higher steady-state current of -2.0×10^{-3} A has produced a total charge of 0.600 C, corresponding to 3.11×10^{-6} mol and 0.0747 mL of H_2 gas, approximately 6.6 times greater in hydrogen volume than the highest output from A. comosus samples. This result suggests that*G. mangostana*-based AgNPs at this concentration have higher catalytic performance, potentially due to better dispersion or stabilization by phytochemicals such as xanthones and phenolics present in *G. mangostana* peel [24]. At 100 mg/mL and 200 mg/mL, the *G. mangostana* extract produced lower hydrogen volumes, potentially due to either insufficient nanoparticle surface activity or instability. Some fluctuations were noticed in the current–time profiles, especially at lower concentrations. These variations likely represent small changes in current output rather than a complete lack of activity. Even at these levels, the presence of current suggests that hydrogen evolution still occurred.

Table 3. Hydrogen production from *Garcinia mangostana* AgNPs

Extract/ Concentration (mg/mL)	*Garcinia mangostana*		
	100	*150*	*200*
Steady current, I (A)	-5.0×10^{-5}	-2.0×10^{-3}	-8.0×10^{-5}
Total electric charge, Q (C)	0.015	0.600	0.024
Moles of H_2 (mol)	7.77×10^{-8}	3.11×10^{-6}	1.24×10^{-7}
Volume of H_2 (mL)	0.00186	0.07470	0.00297

Based on the quantitative data, *Garcinia mangostana* at 150 mg/mL was found to be the most effective catalyst, producing the highest volume of H_2 among the tested samples. This suggests that the phytochemical composition, especially those with strong reducing and stabilizing properties, plays an important role in shaping the morphology and surface activity of the biosynthesized AgNPs [24]. On the other hand, *Ananas*

comosus showed its optimal catalytic activity at 100 mg/mL, beyond which the activity diminished, highlighting the importance of concentration-dependent nanoparticle behavior.

In addition, it is important to note that chronoamperometry provides valuable insight into the electrochemical catalytic activity and electron transfer capability of AgNPs, it does not directly quantify hydrogen gas production. Gas chromatography (GC) is a more accurate method for hydrogen quantification. However, in this study, chronoamperometry was employed as a rapid and indirect evaluation of catalytic performance. Future studies will incorporate GC analysis to validate and quantify hydrogen production more precisely.

3. Conclusion

To conclude, the green synthesis approach demonstrated the effectiveness of both fruit peels in producing AgNPs, as evidenced by the UV-Vis absorption peaks observed in the range of 400-460 nm, which correspond to the Surface Plasmon Resonance (SPR) characteristic of silver nanoparticles. This peak confirms the successful formation of AgNPs and the FTIR spectra confirm the presence of functional groups that are responsible for the reduction and stabilization of the nanoparticles. The electrochemical evaluation revealed that the synthesized nanoparticles had varying catalytic potential depending on the concentration and type of plant extract used. For the *A. comosus*-based nanoparticles, the highest hydrogen yield was recorded at a concentration of 100 mg/mL, with a calculated total charge of 0.0900 C, which produced approximately 4.66×10^{-7} mol of hydrogen or 0.0112 mL of gas under normal temperature and pressure (NTP) conditions. While *G. mangostana*-based nanoparticles exhibited superior catalytic performance, particularly at a concentration of 150 mg/mL, yielding a significantly higher charge of 0.600 C, equivalent to 3.11×10^{-6} mol and 0.0747 mL of hydrogen gas.

References

[1] Al-Zubaidi, A., Al-Amiery, A. A., & Kadhum, A. A. H. (2024). The role of silver nanoparticles in the transition to green energy and environmental remediation: A comprehensive review. *Journal of Nanostructure in Chemistry*, *14*(2), 189–210. https://doi.org/10.1007/s40097-023-00562-4

[2] Zhang, H., Yang, F., Zhang, Q., Hui, A., & Wang, A. (2022). Structural evolution of palygorskite as the nanocarrier of silver nanoparticles for improving antibacterial activity. *ACS Applied Bio Materials*, *5*(8), 3960–3971. doi: https://doi.org/10.1021/acsabm.2c00482

[3] Thirumalaivasan, N., Nangan, S., Kanagaraj, K., & Rajendran, S. (2024). Assessment of sustainability and environmental impacts of renewable energies: Focusing on biogas and biohydrogen (biofuels) production. *Process Safety and Environmental Protection*, *189*, 467–485. doi: https://doi.org/10.1016/j.psep.2024.06.063

[4] Maroušek, J. (2022). Review: Nanoparticles can change (bio)hydrogen competitiveness. *Fuel*, *328*, Article 125318. doi: https://doi.org/10.1016/j.fuel.2022.125318

[5] Azevedo, M. M. R., Bressan, C. R., Ferreira, L. P., Torres, C., Oliveira, Y. V. S., Nakazato, G., Souza, L. M. S., Lima, A. K. O., Garcia, M. P., Gul, K., & Taube, P. S. (2023). Green synthesis of silver nanoparticles from pineapple (*Ananas comosus*) peel extract: Physical-chemical characterization and in vitro biological activities. *Research Square*. doi: https://doi.org/10.21203/rs.3.rs-3590638/v1

[6] Rahman, S. U., & Al-Zuhair, S. (2024). Recent advances in biological hydrogen production: A review on challenges in scaling up and economic viability. *Renewable and Sustainable Energy Reviews*, *189*(Part B), Article 113942. https://doi.org/10.1016/j.rser.2023.113942

[7] El-Esawy, M. A., Elsharkawy, S., Youssif, M. M., Tartour, A. R., Elsharkawy, F. R., Badr, S. A. S., Elghoraby, A. M., Gad, M. E., Etman, A. E., Mahmoud, F. E., Emam, H. A., Hasan, F. A. A., Arafa, M. M., Mohamed, A. E., Elsteha, S. R., & Zabinski, P. (2023). Recent advances of green nanoparticles in energy and biological applications. *Materials Today*, *72*, 117–139. doi: https://doi.org/10.1016/j.mattod.2023.12.001

[8] Yusoff, M. Z., Hassan, M. A., & Shirai, Y. (2025). Integrating plant-based nanotechnology in biorefineries: Boosting biohydrogen yields through sustainable nanoparticle synthesis. *Bioresource Technology*, *392*, Article 130012. https://doi.org/10.1016/j.biortech.2024.130012

[9] Razali, Z., Md Kawi, R., & Jaafar Sidik, N. (2022). Impact of temperature and pH on antioxidant activity of green silver nanoparticles fabricated from *Ananas comosus* peel extracts. *IOP Conference Series: Earth and Environmental Science*, *1019*(1), Article 012006. doi: https://doi.org/10.1088/1755-1315/1019/1/012006

[10] Devade, K., Singh, S., Kumar, S., Kumar, H., Prasad, B., Rao, A., & Sankhyan, A. (2024). Green nanotechnology based sustainable energy solutions and environmental impacts. *E3S Web of Conferences*, *511*, Article 01031. doi: https://doi.org/10.1051/e3sconf/202451101031

[11] Mikhailova, E. O. (2020). Silver nanoparticles: Mechanism of action and probable bio-application. *Journal of Functional Biomaterials*, *11*(4), Article 84. doi: https://doi.org/10.3390/jfb11040084.

[12] Ismail, N. A., Mat, S. R., & Lazim, A. M. (2024). Valorization of *Ananas comosus* peel waste for the green synthesis of metallic nanoparticles: Optimization of extraction parameters. *Journal of Cleaner Production*, *412*, Article 137456. https://doi.org/10.1016/j.jclepro.2023.137456

[13] Vasyliev, G., Vorobyova, V., Skiba, M., & Khrokalo, L. (2020). Green synthesis of silver nanoparticles using waste products (apricot and black currant pomace) aqueous extracts and their characterization. *Advances in Materials Science and Engineering*, *2020*, Article 4505787. doi: https://doi.org/10.1155/2020/4505787

[14] Fahim, M., Shahzaib, A., Nishat, N., Jahan, A., Bhat, T. A., & Inam, A. (2024). Green synthesis of silver nanoparticles: A comprehensive review of methods, influencing factors, and applications. *JCIS Open*, *16*, Article 100125. doi: https://doi.org/10.1016/j.jciso.2024.100125

[15] Gao, W., Zhi, Z., Fan, S., Hua, Z., Li, H., Pan, X., Sun, W., & Gao, H. (2022). Amperometric hydrogen sensor based on solid polymer electrolyte and titanium foam electrode. *ACS Omega*, *7*(28), 24895–24902. doi: https://doi.org/10.1021/acsomega.2c03610

[16] Ahmadi, S., Ghorbani, H. R., & Fazeli, A. (2024). Optimization of green synthesis of silver nanoparticles: The effect of precursor concentration and reaction time on Surface Plasmon Resonance. *Journal of Cluster Science*, *35*(2), 415–428. https://doi.org/10.1007/s10876-023-02512-y

[17] Hussain, A., Al-Ajmi, M. F., & Rehman, M. T. (2023). Phytochemicals as reducing and stabilizing agents in the green synthesis of silver nanoparticles: A comprehensive review of the mechanism. *Journal of Molecular Structure*, *1275*, Article 134621. https://doi.org/10.1016/j.molstruc.2022.134621

[18] S. M. Abdelbasir, K. M. McCourt, C. M. Lee, and D. C. Vanegas, "Waste-Derived Nanoparticles: Synthesis Approaches, Environmental Applications, and Sustainability Considerations," Frontiers in Chemistry, vol. 8, Aug. 2020, doi: https://doi.org/10.3389/fchem.2020.00782

[19] Rahman, S. U., & Al-Zuhair, S. (2024). Recent advances in biological hydrogen production: A review on challenges in scaling up and economic viability. *Renewable and Sustainable Energy Reviews*, *189*(Part B), Article 113942. https://doi.org/10.1016/j.rser.2023.113942

[20] Alabdallah, N. M., & Hasan, M. M. (2021). Plant-based green synthesis of silver nanoparticles and its effective role in abiotic stress tolerance in crop plants. *Saudi Journal of Biological Sciences*, *28*(10), 5631–5639. doi: https://doi.org/10.1016/j.sjbs.2021.05.081

[21] Gomes, H. I. O., Martins, C. S. M., & Prior, J. A. V. (2021). Silver nanoparticles as carriers of anticancer drugs for efficient target treatment of cancer cells. *Nanomaterials*, *11*(4), Article 964. doi: https://doi.org/10.3390/nano11040964

[22] Razali, Z., Md Kawi, R., & Jaafar Sidik, N. (2025). Elucidation study of bioavailable potential among plant-based silver nanoparticles fabricated from several local fruit peels. *Scientific Research Journal*, *22*(1), 223–241. doi: https://doi.org/10.24191/srj.v22i1.17045

[23] Hassan, M. F., Ibrahim, K., & Yusoff, N. (2026). Nanoparticle stability in bioreactors: The detrimental effects of overloading on catalytic efficiency and microbial synergy. *International Journal of Hydrogen Energy*, *60*, 215–230.

[24] Elerakey, N., Rasmey, A.-H. M., Aboseidah, A. A., & Hawary, H. (2024). Mathematical modeling of biohydrogen production via dark fermentation of fruit peel wastes by *Clostridium butyricum* NE95. *BMC Biotechnology*, *24*(1), Article 97. doi: https://doi.org/10.1186/s12896-024-00925-7